Successive Gas-Solid Reaction Model for the Hydrogen Reduction of Cuprous Sulfide in the Presence of Lime

H. Y. SOHN and S. WON

As an alternative to conventional smelting processes for producing metals from sulfide ores, which suffer from SO_2 emission problems, direct reduction in the presence of lime has in recent years attracted much attention. In this work, a mathematical model of successive gas-solid reactions in a porous pellet has been applied to the hydrogen reduction of cuprous sulfide (Cu_2S) in the presence of lime. The model has been formulated by incorporating the intrinsic kinetics of the individual reactions obtained from separate experiments, and compared with the experimental results on the hydrogen reduction of chalcocite mixed with lime particles. The model predictions were in good agreement with experimental measurements of the overall rate of reaction and the degree of sulfur fixation over a wide range of experimental conditions. The mathematical model not only can predict the performance of a given system but also enables one to design the optimum pellet properties and reaction conditions in terms of the reaction rate and sulfur fixation.

I. INTRODUCTION

THE conventional pyrometallurgical processes, smelting or roasting, for treating sulfide minerals produce sulfur dioxide gas which causes pollution problems. An alternative process, which has attracted much attention, is the direct hydrogen reduction of metal sulfides in the presence of lime.[1-7] This reaction can be represented by the following two successive gas-solid reactions:

$$H_2(g) + Me_xS(s) = H_2S(g) + xMe(s) \quad [1]$$

$$H_2S(g) + CaO(s) = H_2O(g) + CaS(s) \quad [2]$$

$$H_2(g) + Me_xS(s) + CaO(s) = H_2O(g) + xMe(s) + CaS(s) \quad [3]$$

Reaction [2] has a large equilibrium constant ($\sim 10^3$ in the temperature range of interest) and therefore leaves very little H_2S gas in the gas phase at equilibrium. Furthermore, it improves the otherwise unfavorable thermodynamics of reaction [1] by removing hydrogen sulfide from the gas phase.

The objective of the present investigation was to develop a mathematical model for reaction [3] which takes place in a porous pellet made up of a uniform mixture of chalcocite (Cu_2S) and lime particles, and to compare the model predictions with experimental measurements in terms of the sulfide reduction and the sulfur fixation by lime.

In 1977, Sohn and Rajamani[5] proposed a model for isothermal, successive gas-solid reactions in a porous pellet, which took into consideration the effects of the relative amounts of the solids, grain sizes, and the pellet size and porosity. However, the study was entirely theoretical, and the mathematical model presented therein was formulated in general terms such that specific details must be incorporated when applied to an actual system. The model presented in this paper has been specifically formulated for the hydrogen reduction of chalcocite in the presence of lime with the objective of systematically representing the system behaviors, including the rates of component reactions and the degree of sulfur fixation.

The only mathematical modeling effort on this reaction system other than those by Sohn and Rajamani[5,8] is that by Fahim *et al.*[9] Although it contains many similar features, their model has an important shortcoming in that the hydrogen sulfide produced from the metal sulfide is assumed to react quantitatively with the lime. Thus, with an amount of lime equal to or greater than the stoichiometric value, all the hydrogen sulfide produced is assumed to be captured by lime. This makes their model incapable of computing the degree of sulfur fixation which varies with the pellet structure and reaction condition, as observed experimentally by many investigators.[1,3,7] This also results in incorrect representation of the local hydrogen sulfide concentration which has a serious effect on the prediction of the rate of reaction [1], because this reaction has a very small equilibrium constant and thus its rate depends very strongly on H_2S concentration. In their work, the model results for the rate of reduction of sulfide was fitted to their experimental results by using the effective diffusivity as an adjustable parameter. Perhaps because of the above assumption, the resulting best-fit values of effective diffusivities showed considerable scatter and were rather inconsistent with the porosity of the pellet.[10]

II. MODEL FORMULATION

The successive gas-solid reactions exemplified by reactions [1] through [3] can be written in the following general form:

$$A(g) + bB(s) = cC(g) + fF(s) \quad [4]$$

$$C(g) + dD(s) = eE(g) + gG(s) \quad [5]$$

For the hydrogen reduction of metal sulfides in the presence of lime, $c = e = 1$; *i.e.*, there is no net change in the number of moles of gaseous species.

Let us consider a porous pellet of volume V_p and superficial surface area A_p, made up of a uniform mixture of

H. Y. SOHN is Professor in the Department of Metallurgy and Metallurgical Engineering, University of Utah, Salt Lake City, UT 84112-1183. S. WON, formerly Graduate Student in the Department of Metallurgy and Metallurgical Engineering, University of Utah, is now Senior Metallurgist with Cyprus Metallurgical Processes Corporation, 800 East Pima Mine Road, Tucson, AZ 85725.

Manuscript submitted November 20, 1984

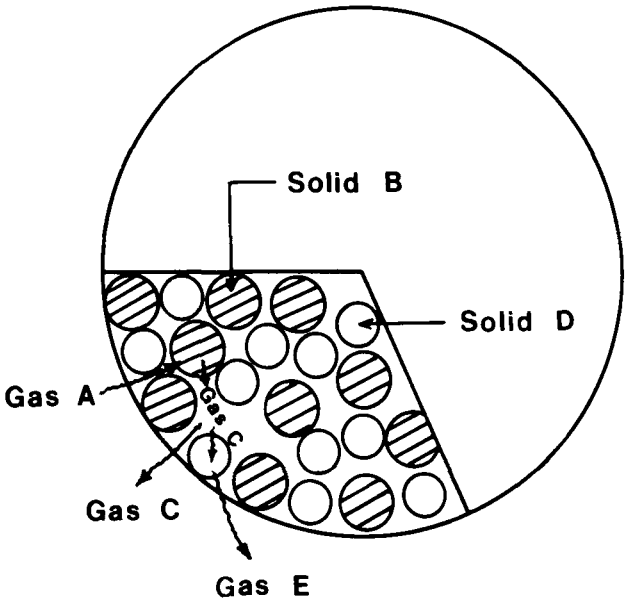

Fig. 1 — Schematic representation of the pellet made up of a uniform mixture of solids B and D

grains of solids B (chalcocite) and D (lime), as shown in Figure 1. The reduction proceeds in the following manner: Gas A (hydrogen) is transferred from the bulk gas stream to the surface of the pellet, diffuses between the grains, and reacts with chalcocite. The product gas C (hydrogen sulfide) diffuses back and reacts with lime forming calcium sulfide and gas E (water vapor). Water vapor and some unreacted hydrogen sulfide diffuse out to the surface of the pellet and then into the bulk gas stream.

The following assumptions will be used in the formulation:

(1) The physical structure of the pellet is macroscopically uniform and unchanged by the reaction.
(2) The system is isothermal.
(3) The pseudosteady-state approximation is appropriate for describing the concentrations of gaseous species within the pellet.
(4) Diffusion of the gaseous species through the product layer of the individual grain is fast and thus does not offer any resistance to the overall rate.

It may be worthwhile to comment briefly on the appropriateness of these assumptions. Assumption (1) is rather restrictive; nonetheless it is thought to be valid for a range of experimental conditions especially in the presence of excess lime. Assumption (2) has been verified experimentally in this work, as expected of the reaction under study which involves a small overall heat of reaction. Assumption (3) is well established for gas-solid reactions.[11,12] Assumption (4) is thought to be valid for fine particles used in this study.

Within the framework of the above assumptions, the problem may be stated by combining expressions for the conservation of the gaseous species with mass balances for the reaction of the solids. The conservation of the gaseous species is given by the following:

$$D_{eA}\nabla^2 C_A - v_1 = 0 \qquad [6]$$

$$D_{eC}\nabla^2 C_C + v_1 - v_2 = 0 \qquad [7]$$

$$D_{eE}\nabla^2 C_E + v_2 = 0 \qquad [8]$$

where D_{eA}, D_{eC}, and D_{eE} are the effective diffusivities inside the pellet; C_A, C_C, and C_E are the molar concentrations of gas species; and v_1 and v_2 are the local net forward rates per unit pellet volume of reactions [4] and [5], respectively. A more rigorous formulation of the problem would require writing these conservation equations using the Maxwell-Stefan expressions for the diffusional process involving a multicomponent mixture. For mathematical simplicity, we used the above expressions using the pseudobinary diffusivities. This is thought to be appropriate because in most cases the diffusing species H_2S and H_2O are at low concentrations in H_2.

From the experimental results,[13,14] reactions [1] for Cu_2S and [2] were found to be of first order with respect to the concentrations of hydrogen and hydrogen sulfide, respectively, in the forward direction. Therefore, these reactions may be considered to be first order with respect to the gases in both the forward and the reverse directions because equal moles of gaseous species are involved in both directions of each reaction. The hydrogen reduction of chalcocite was determined experimentally to follow the nucleation and growth kinetics,[13] and the reaction of hydrogen sulfide with lime was found to be represented by the pore-blocking model.[13,14] The kinetic expression for each reaction can be written as follows:

For the nucleation and growth kinetics,

$$bk_1(C_A - C_C/K_1)t = [-\ln(1 - \omega_B)]^{1/m} \equiv f(\omega_B) \qquad [9]$$

and for the pore-blocking model,

$$d(k_2/\lambda)(C_C - C_E/K_2)t = \exp(\omega_D/\lambda) - 1 \equiv g(\omega_D) \qquad [10]$$

where m and λ are constants, ω_B and ω_D are the local values of the fractional conversion of the solid reactants B and D, respectively, k_1 and k_2 are forward reaction rate constants, and K_1 and K_2 are the equilibrium constants for reactions [4] and [5], respectively. From Eqs. [9] and [10], the local rates of reaction of the solids can be obtained as:

$$\frac{\partial \omega_B}{\partial t} = \frac{bk_1}{f'(\omega_B)}(C_A - C_C/K_1) \qquad [11]$$

$$\frac{\partial \omega_D}{\partial t} = \frac{dk_2/\lambda}{g'(\omega_D)}(C_C - C_E/K_2) \qquad [12]$$

where prime designates the derivative with respect to ω_B or ω_D.

The expression for v_1 and v_2 can be obtained by considering the stoichiometry and the initial concentrations of the solids, as given below:

$$v_1 = \frac{\alpha_B \rho_B}{b}\frac{\partial \omega_B}{\partial t} = \frac{\alpha_B \rho_B k_1}{f'(\omega_B)}(C_A - C_C/K_1) \qquad [13]$$

$$v_2 = \frac{\alpha_D \rho_D}{d}\frac{\partial \omega_D}{\partial t} = \frac{\alpha_D \rho_D k_2/\lambda}{g'(\omega_D)}(C_C - C_E/K_2) \qquad [14]$$

where α_B and α_D are the fractions of pellet volume initially occupied by the solids B and D, respectively, and ρ_B and ρ_D are the true molar densities of B and D, respectively.

Equations [6] through [14] represent the complete statement of the problem. The solution of these equations with appropriate initial and boundary conditions will yield the profiles of gaseous and solid species, the conversions of the solids at any time, and the fraction of the gas C produced that reacts with solid D. The last item is an important factor for the reaction of sulfide minerals, because it represents the fraction of the sulfur-containing gas captured by lime.

Since the concentrations of hydrogen sulfide and water in the region of the pellet where substantial concentration gradients exist are rather low, as will be shown below (Figure 7), the molecular diffusion may be considered as two separate binary diffusion processes between H_2 and H_2S and between H_2 and H_2O. Furthermore, we shall assume these two binary diffusivities to be equal. This is not a critical assumption, but it simplifies the mathematics somewhat without much loss of accuracy, as verified elsewhere.[13]

With this additional assumption, Eqs. [6] through [14] may be written in dimensionless forms, as follows:

$$\nabla^{*2}\psi_A - 2F_p\hat{\sigma}_B^2\frac{\psi_A}{f'(\omega_B)} + 2F_p\hat{\sigma}_D^2\left[\frac{K_2}{K_1(1+K_2)}\right]\frac{\psi_C}{g'(\omega_D)} = 0 \quad [15]$$

$$\nabla^{*2}\psi_C - 2F_p\hat{\sigma}_D^2\frac{\psi_C}{g'(\omega_D)} + 2F_p\hat{\sigma}_B^2\left[\frac{K_1}{1+K_1}\right]\frac{\psi_A}{f'(\omega_B)} = 0 \quad [16]$$

and

$$\frac{\partial\omega_B}{\partial t^*} = \frac{\psi_A}{f'(\omega_B)} \quad [17]$$

$$\frac{\partial\omega_D}{\partial t^*} = \beta\frac{\psi_C}{g'(\omega_D)} \quad [18]$$

The dimensionless variables and parameters introduced in the above equations are defined as follows: ∇^{*2} is the Laplacian operator with η as the position coordinate with

$$\eta \equiv \frac{A_p R}{F_p V_p} \quad [19]$$

where R is the distance from the center of symmetry within the pellet, and F_p is the shape factor for the pellet:

$$\psi_A \equiv \frac{C_A - C_C/K_1}{C_{Ab} - C_{Cb}/K_1} \quad [20]$$

$$\psi_C \equiv \frac{C_C - C_E/K_2}{C_{Ab} - C_{Cb}/K_1} \quad [21]$$

and

$$\hat{\sigma}_B \equiv \frac{V_p}{A_p}\left[\frac{\alpha_B\rho_B F_p k_1}{2D_e}\left(1 + \frac{1}{K_1}\right)\right]^{1/2} \quad [22]$$

$$\hat{\sigma}_D \equiv \frac{V_p}{A_p}\left[\frac{\alpha_D\rho_D F_p k_2/\lambda}{2D_e}\left(1 + \frac{1}{K_2}\right)\right]^{1/2} \quad [23]$$

which represent the relative capacities for chemical reaction and intrapellet diffusion. These are parameters which have a role akin to that of the Thiele modulus in heterogeneous catalysis. The considerable advantages for this particular definition of this group in analyzing gas-solid reactions of various types and complexities have been repeatedly demonstrated and discussed.[15-19] It is noted that:

$$\hat{\sigma}_D^2 = \gamma\beta\hat{\sigma}_B^2\left[\frac{K_1(1+K_2)}{K_2(1+K_1)}\right] \quad [24]$$

where

$$\gamma \equiv \frac{b\alpha_D\rho_D}{d\alpha_B\rho_B} \quad [25]$$

which is a measure of the relative molar quantity of the two solids in the pellet, and

$$\beta = \frac{dk_2/\lambda}{bk_1} \quad [26]$$

which represents the ratio of the reactivities of the two reactant solids. Finally, the dimensionless time is defined as

$$t^* \equiv bk_1(C_{Ab} - C_{Cb}/K_1)t. \quad [27]$$

The boundary and initial conditions for Eqs. [15] through [18] are readily written as follows:

$$\frac{\partial\psi_A}{\partial\eta} = \frac{\partial\psi_C}{\partial\eta} = 0 \quad \text{at} \quad \eta = 0 \quad [28]$$

$$\left.\begin{aligned}\frac{\partial\psi_A}{\partial\eta} &= \mathrm{Sh}^*(1 - \psi_A) \quad [29a]\\ \frac{\partial\psi_C}{\partial\eta} &= \mathrm{Sh}^*(\psi_{Cb} - \psi_C) \quad [29b]\end{aligned}\right\} \quad \text{at} \quad \eta = 1$$

and

$$\omega_B = \omega_D = 0 \quad \text{at} \quad t^* = 0 \quad [30]$$

where

$$\mathrm{Sh}^* = \frac{k_m}{D_e}\left(\frac{F_p V_p}{A_p}\right) = \mathrm{Sh}\frac{D_M}{D_e} \quad [31]$$

The solution of Eqs. [15] through [18], together with the boundary and initial conditions [28] through [30], yields ψ_A, ψ_C, ω_B, and ω_D as functions of η and t^*. For most practical purposes, however, the overall conversion of each solid is of greater interest. In terms of the parameters used in the formulation these quantities may be obtained from the following relationships:

$$X_B = \frac{\int_0^1 \alpha_B\eta^{F_p-1}\omega_B\,d\eta}{\int_0^1 \alpha_B\eta^{F_p-1}\,d\eta} \quad [32]$$

$$X_D = \frac{\int_0^1 \alpha_D\eta^{F_p-1}\omega_D\,d\eta}{\int_0^1 \alpha_D\eta^{F_p-1}\,d\eta} \quad [33]$$

Another important factor, especially in the treatment of sulfide minerals, as noted earlier, is the fraction of the gas C (H_2S) produced from the solid B (Cu_2S) that is captured by the solid D (CaO). From the consideration of stoichiometry, this factor may be obtained from the following

relationship:

$$F = \frac{\text{moles of } C \text{ reacted with } D}{\text{moles of } C \text{ produced by } B \text{ reacted}}$$

$$= \frac{\alpha_D \rho_D X_D / d}{\alpha_B \rho_B X_B / b}$$

$$= \frac{\gamma X_D}{X_B} \qquad [34]$$

From the above formulation, by writing the governing equations in dimensionless forms, it is noted that the characteristic parameters that define the system, that is, the species profiles, the conversions of solid, and the fraction of sulfur fixed in solid, are related to time by just three parameters—$\hat{\sigma}_B$, γ, and β. The computational economy in investigating the effects of certain variables, resulting from the reduction of the number of parameters, needs no further elaboration.

III. SOLUTION PROCEDURE

Compared with a single gas-solid reaction, the complete analytical solution of the system of a successive gas-solid reaction is much more complex, even when possible. For most systems, analytical solutions are not possible. Therefore, numerical solution was obtained throughout this work.

The procedure for numerical solution is as follows. At $t^* = 0$, $\omega_B = \omega_D = 0$ from Eq. [30]. With these values, Eqs. [15] and [16] are solved for ψ_A and ψ_C as functions of η, using boundary conditions [28] and [29]. This system of two-point boundary value equations was solved using the technique described by Newman.[20] Using the values of ψ_A and ψ_C at $t^* = 0$ thus obtained, ω_B and ω_D at $t^* = \Delta t^*$ are computed from Eqs. [17] and [18] using the fourth-order Runge-Kutta method. New values of ω_B and ω_D are obtained which can be used to solve Eqs. [15] and [16] to give ψ_A and ψ_C *vs* η at $t^* = \Delta t^*$. This procedure is repeated for increasing time steps. The conversion of the solids at any time are obtained by a Simpson's rule integration using Eqs. [32] and [33], and F (the fraction of gas C fixed) may be calculated by Eq. [34]. From physical reasoning it is noted that ψ cannot be negative and ω cannot become negative or greater than one.

The numerical solution should approach the analytical results closely when its asymptotic behaviors are examined. This fact was used to check the accuracy of the numerical solution.

When $\hat{\sigma}_B$ approaches zero, *i.e.*, the pore diffusion is extremely fast compared with the intrinsic kinetics, the gaseous reactant concentrations are uniform throughout the pellet and are equal to those in the bulk, and ω_B and ω_D are independent of η. Under these conditions, Eqs. [17] and [18] are readily integrated and $X_B = \omega_B$ from Eq. [32] and $X_D = \omega_D$ from Eq. [33]. The relationships between X's and t^* are then given by

$$t^* = [-\ln(1 - X_B)]^{1/m} \qquad [35]$$

which was confirmed by numerical solution with $\hat{\sigma}_B = 0.01$ and

$$t^* = -\frac{1}{\beta K_1}[\exp(X_d/\lambda) - 1] \qquad [36]$$

which was verified with $\hat{\sigma}_D = 0.01$ using $\psi_A = 1$ and $\psi_C = -K_1$ at $\eta = 1$ (corresponding to $C_{Ab} = C_{Eb} = 0$).

On the other hand, when $\hat{\sigma}_B$ approaches infinity, reaction occurs mostly in a narrow zone between the unreacted core and the completely reacted layer. The concentration driving force for reaction, $(C_A - C_C/K_1)$, drops to nearly zero at this reaction zone, and the diffusion through the product layer controls the overall rate. Under these conditions, the type of intrinsic kinetics does not affect the overall rate, and two extreme cases were examined: first, the hydrogen reduction of chalcocite in a pellet mixed with an inert material ($\beta = 0$), and second, the reduction of chalcocite in the presence of highly excessive amounts of lime ($\gamma = 50$). For the first case, the conversion-time relationship is given by:

$$\frac{t^*}{\hat{\sigma}_B^2} = 1 + 2(1 - X_B) - 3(1 - X_B)^{2/3}$$

$$\equiv P_{F_p}(X_B) \qquad [37]$$

which was approximated, when $\hat{\sigma}_B$ becomes greater than three. For the second case, assuming that equilibrium condition prevails at the reaction interfaces of chalcocite and lime particles, the conversion-time relationship can be derived as follows:

$$\frac{t^*}{\hat{\sigma}_B^2} = \frac{1 + K_1 + K_1 K_2}{(1 + K_1)(1 + K_2)} P_{F_p}(X_B) \qquad [38]$$

which was also verified, when $\hat{\sigma}_B$ approaches 10.

IV. EXPERIMENTAL

Spherical pellets were prepared by isostatically pressing mixtures of fine Cu_2S and CaO particles. The pellets were placed in a platinum-wire basket which was hung on one arm of a continuously recording electrobalance. The reaction was followed by the continuous weight loss during the reaction with hydrogen. Other details of the materials and experimental procedure can be found elsewhere.[13,21]

V. PARAMETERS REQUIRED FOR THE MODEL

All the measurements for the hydrogen reduction of chalcocite in the presence of lime were made under the condition of a negligible effect of external mass transfer.[13,21] The following parameters are required for the model in order to calculate the extent of reaction and the degree of sulfur fixation as functions of time:

(i) diameter of the pellet,
(ii) temperature of the system,
(iii) the reactant gas concentration in the bulk gas stream (C_{Ab}),
(iv) the true molar density of the solid reactants (ρ_B, ρ_D),
(v) the molar mixing ratio of the solid reactants (γ),
(vi) porosity of the pellet (ε),
(vii) the fractions of the pellet volume occupied by the solids (α_B, α_D),
(viii) the equilibrium constants of reactions [1] and [2] (K_1, K_2),
(ix) the reaction rate constants for reactions [1] and [2] (k_1, k_2), and λ for the latter, and
(x) the effective diffusivities of hydrogen, hydrogen sulfide, and water vapor in the pellet (D_e).

Measurements of (i), (ii), (iv), and (vi) have already been discussed in References 13 and 21 and will be given no further attention here. The concentration of the bulk gas can be calculated from the ideal gas law. Calculations of (vii) were made using the initially known value of (v) and (vi). The values of (viii) were obtained from the literature.[22,23]

The kinetics of the individual reactions [1] and [2] have been studied separately using the same materials and the rate parameters obtained.[13,14] The reader is referred to these references for the details involved in the measurement of k_1, k_2, and λ. In these studies, to ensure measurement of the intrinsic rate constants, the experimental runs were carried out under such conditions that the effect of the physical properties of the reactor system was absent.

The kinetics of reaction [1] for the synthetic cuprous sulfide used in this work was determined using porous pressed disks and loose particles.[13] The rate constant obtained for the pressed disks was greater by a factor of about two than for the latter. The rate expression for the pressed porous disks was used in the model prediction because the mixture pellet was also prepared by pressing the particles. The expression for k_1 thus obtained is

$$k_1 = 4.085 \times 10^6 \exp(-11070/T) \text{ cm}^3/(\text{mol} \cdot \text{s}) \quad \text{for } Cu_2S \qquad [39]$$

The expression for k_2 will be discussed in the following section. The parameter λ was found to depend on temperature,[13] as shown in Figure 2.

The phenomenon of gaseous diffusion in porous media has been extensively studied by a number of workers. It is possible to predict a value from a number of models which are available in the literature.[24,25,26] One of the few completely predictive models is the "random pore model" proposed by Wakao and Smith.[24] This model is designed to describe diffusion of gases in pellets prepared by compressing porous powders. Since lime, which has a theoretical porosity of 56.6 pct, constitutes a large portion of the pellets, the application of this model in predicting the effective diffusivity seemed to be reasonable. When the pore size distribution is mono-dispersed as mostly observed in this study,[13] the effective diffusivity can be written as:

$$D_e = \frac{\varepsilon^2}{1/D_{H_2\text{-}H_2O} + 1/D_K} \qquad [40]$$

when H_2S concentration within a mixture pellet is expected to be very small, where $D_{H_2\text{-}H_2O}$ is the molecular diffusivity of the H_2-H_2O system, and D_K is the average Knudsen diffusivity given by:

$$D_K = 0.97 r_c \sqrt{T/M} \qquad [41]$$

where r_c is the critical pore radius in μm, T temperature in K, and M the average molecular weight of the gas mixture. The critical pore radius is that pore radius corresponding to the point of inflection in the pore volume-*vs*-pore radius curve obtained in the mercury penetration porosimetry.

The molecular diffusivity was calculated by the Chapman-Enskog formula,[27] and the Knudsen diffusivity was obtained using the critical radius determined from the pore size distribution of *reacted mixture pellets*. The values of $D_{H_2\text{-}H_2O}$, D_K, and D_e thus obtained are listed in Table I. Knudsen diffusion will occur when the diffusing gas has a mean free path larger than the mean pore diameters in the pellet. At 600 °C, the mean free path of hydrogen and water vapor are 0.66 and 0.48 μm, respectively, and will increase at higher temperature. These values are larger than the mean pore diameters (0.2 to 0.46 μm) obtained in this work. Thus it is reasonable to assume that Knudsen diffusion plays an important role in determining the overall diffusivity in the pellet.

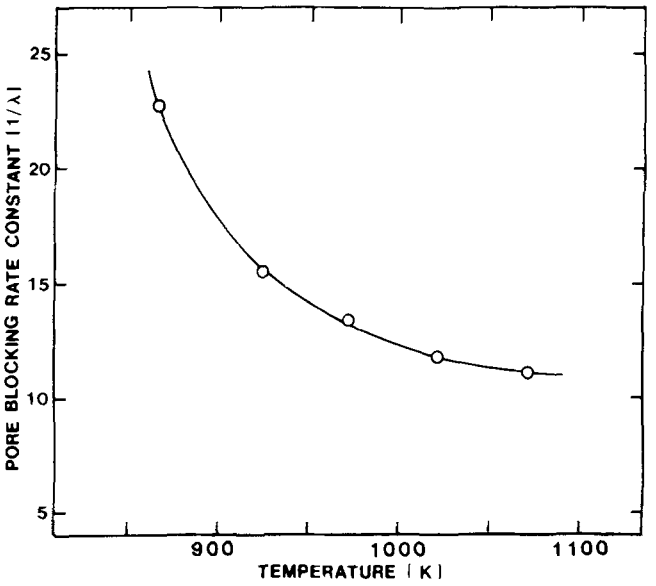

Fig. 2—Experimentally determined pore-blocking rate constant ($1/\lambda$) as a function of temperature.

In Eq. [40] and in the development of the mathematical model, the molecular diffusivity is based on binary gas diffusion of hydrogen and water vapor, and the effective diffusivity of each gas component is assumed to be equal.

VI. COMPARISON OF EXPERIMENTAL RESULTS WITH COMPUTED RESULTS USING THE MODEL

When a mixture of metal sulfide and lime is reacted with hydrogen, water vapor and hydrogen sulfide diffuse out of the mixture into the bulk stream. The ratio of the amount of hydrogen sulfide which is captured to that which escapes depends on the amount of lime used, reaction temperature, pellet size, and effective diffusivity. If the amount of hydrogen sulfide escaping from the pellet could be accurately determined, the conversion of the sulfide and lime could be computed from the weight change at any time. It is, however, quite difficult to do this because the partial pressure of hydrogen sulfide in this system is very low. Furthermore, a rather high flow rate of hydrogen, used in the reactor to eliminate the effect of external mass transfer, and the inert gas, used to flush the balance, further dilute the H_2S concentration. In this work, therefore, theoretical predictions are compared with the experimental results in terms of the fractional weight loss (F.W.L.) and the overall sulfur fixation. The fractional weight loss is obtained by dividing the weight loss at a particular time by the initial weight of the pellet rather than by the final weight change. This was done because the final weight change in this reaction system depends on the degree of sulfur fixation by lime. When the

Table I. Estimation of Effective Diffusivities*

Effect of Temperature					
T (°C)	r_c (μm)	ε	$D_{H_2\text{-}H_2O}$ (cm^2/s)	D_K (cm^2/s)	D_e (cm^2/s)
600	0.108	0.342	6.334	0.979	0.099
650	0.120	0.338	6.934	1.118	0.110
700	0.100	0.367	7.614	0.957	0.114
750	0.110	0.334	8.371	1.079	0.107
Effect of Porosity (700 °C)					
γ	r_c (μm)	ε	$D_{H_2\text{-}H_2O}$ (cm^2/s)	D_K (cm^2/s)	D_e (cm^2/s)
3	0.190	0.482	7.614	1.818	0.340
3	0.230	0.531	7.614	2.201	0.481
Effect of Mixing Ratio (700 °C)					
γ	r_c (μm)	ε	$D_{H_2\text{-}H_2O}$ (cm^2/s)	D_K (cm^2/s)	D_e (cm^2/s)
1	0.100	0.266	7.614	0.957	0.060
2	0.162	0.315	7.614	1.550	0.127
4	0.100	0.348	7.614	0.957	0.103
Effect of Pellet Size (700 °C)					
D_p (cm)	r_c (μm)	ε	$D_{H_2\text{-}H_2O}$ (cm^2/s)	D_K (cm^2/s)	D_e (cm^2/s)
0.611	0.185	0.346	7.614	1.770	0.127
0.816	0.167	0.345	7.614	1.598	0.157
0.953	0.180	0.351	7.614	1.722	0.173

*These values were obtained using the physical properties of the mixture pellets reacted under the actual experimental conditions (Figures 4, 6 to 8)

metal sulfide in a pellet is completely reduced, the predicted sulfur fixation (F) is compared with the experimental value which can be computed from the measured final weight change.[13,21]

The theoretical predictions were obtained by introducing kinetic and physical parameters of each pellet into the computer program. The predicted values were lower than the experimental results when the following expression of k_2 obtained for dry lime was used:[14]

$$k_2 = k_{20} \exp(-9160/T) \text{ cm}^3/(\text{mol} \cdot \text{s}) \qquad [42]$$

Although dry lime was used to prepare the pellet, lime absorbed some moisture during the preparation of the pellets, which changed its reactivity.[15] Therefore, it was decided to use the preexponential factor of the rate constant k_2, obtained by matching the predicted sulfur fixation with the total fixation obtained experimentally at 700 °C for the pellet of mixing ratio of one, for which the effect of reactivity ratio of two solids is significant. Figure 3 shows the effect of different preexponential factors (k_{20}) on the model predictions. For the value of k_{20} (= 2.87×10^7 cm^3/(mol · s)) experimentally determined for reaction [2] with dry with lime (0.9 pct initial moisture), the model predicted only 31.3 pct of sulfur fixed in lime (compared with the experimental value of 64.3 pct) and substantially underestimated the extent of reaction. The value of k_{20} which enabled the model to predict correctly the final sulfur fixation for this case was 5.68×10^9 cm^3/(mol · s). With this value of k_{20}, the model could also predict the experimental results of fractional weight loss *vs* time quite satisfactorily.

The adjusted value of k_{20} corresponds to that for lime particles with an initial moisture content of 13.0 pct.[14] This suggests that, during the preparation of the mixture pellet, the initially dry (0.9 pct moisture) lime absorbed moisture. The moisture absorbed by the lime affects only the reactivity of lime and not the weight change due to the reduction of the sulfide, because the pellet was completely dried under flowing helium before hydrogen was introduced.[13,21] In retrospect, it would have been of interest to determine the moisture content of the pellet just before the reaction. This was not done because the model predictions were computed after the experimental measurements had been completed.

The model was tested for different temperatures by using the adjusted value of the preexponential factor and the activation energy which was obtained experimentally for reaction [2]. This procedure resulted in a reasonable agreement. Therefore, the rate constant for reaction [2] within a mixture pellet was calculated using the following equation:

$$k_2 = 5.68 \times 10^9 \exp(-9160/T) \text{ cm}^3/(\text{mol} \cdot \text{s}) \qquad [43]$$

The results of model predictions are presented together with the experimental data at various conditions in the following sections.

A. *Effect of Temperature*

The experimental results were in good agreement with the theoretical predictions, as shown in Figures 4(a) through (d), except for the runs at 750 °C in which extensive sintering occurred in the later stage of the reaction.[13] This structural change violates one of the assumptions used in the model, and thus it is not surprising that agreement is somewhat less satisfactory at 750 °C.

The predicted values and experimental data of sulfur fixation are also given in Figures 4(a) through (d) at different temperatures. The model is able to predict the degree of sulfur fixation within ±6.0 pct of the experimental results. As the diffusional effect became relatively greater with increasing temperature, the sulfur fixation increased.

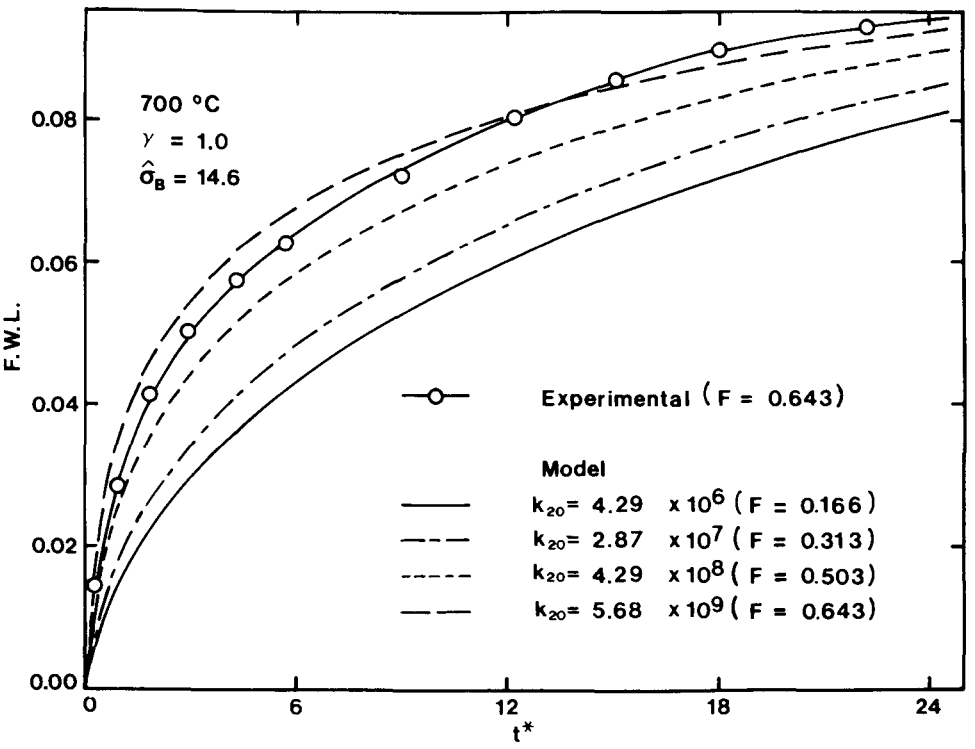

Fig 3—Determination of the best-fit value of k_{20} for $\gamma = 1.0$ at 700 °C

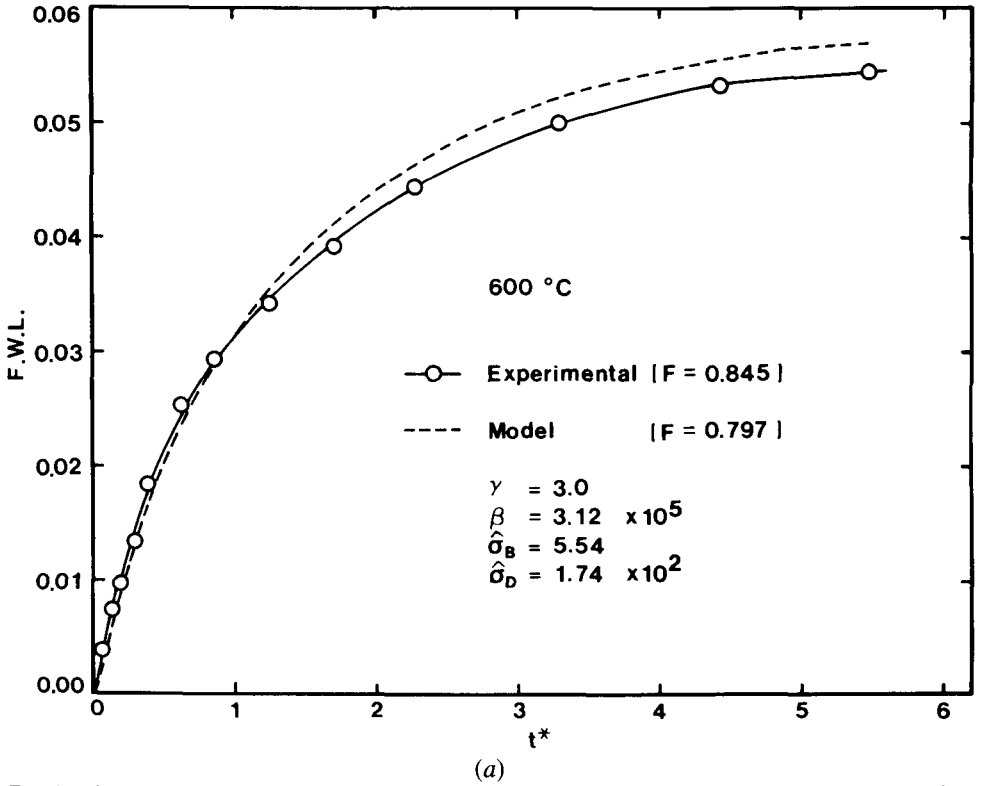

(*a*)

Fig. 4—Comparison of the model predictions with experimental results at various temperatures. (*a*) 600 °C, (*b*) 650 °C, (*c*) 700 °C, and (*d*) 750 °C.

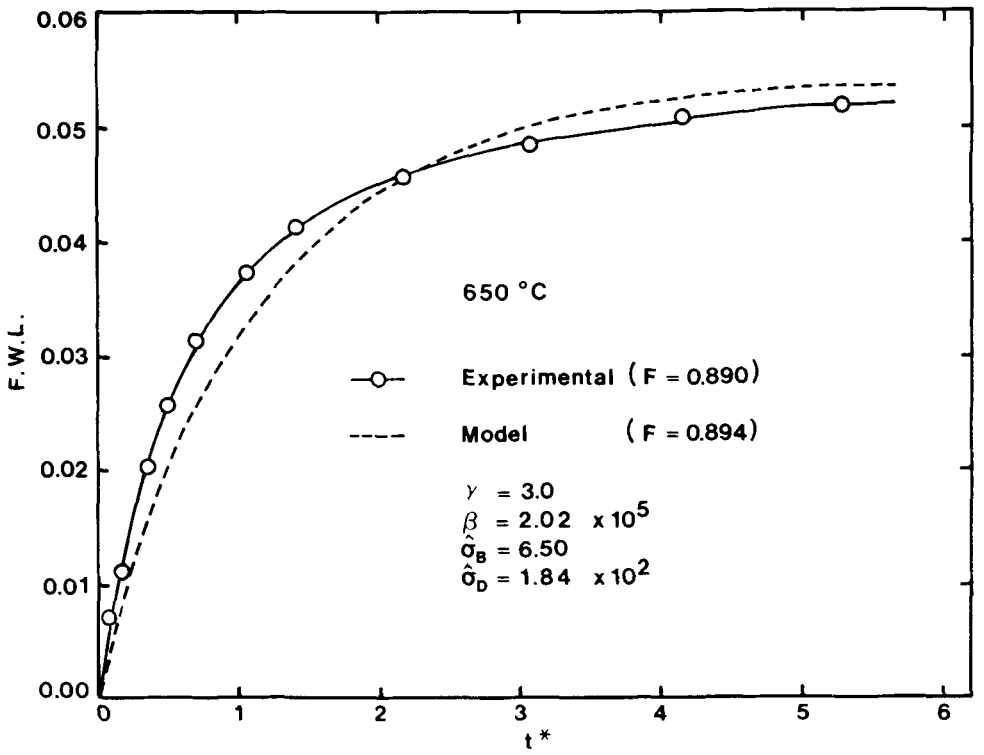

(*b*)

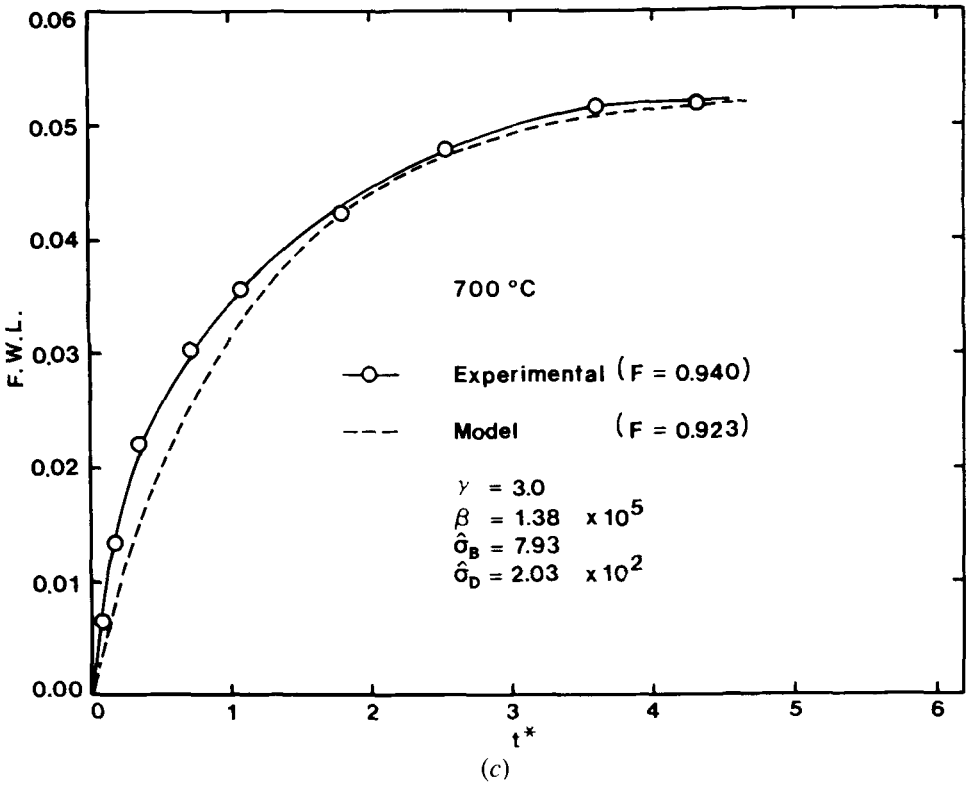

(*c*)

Fig. 4—Comparison of the model predictions with experimental results at various temperatures: (*a*) 600 °C, (*b*) 650 °C, (*c*) 700 °C, and (*d*) 750 °C

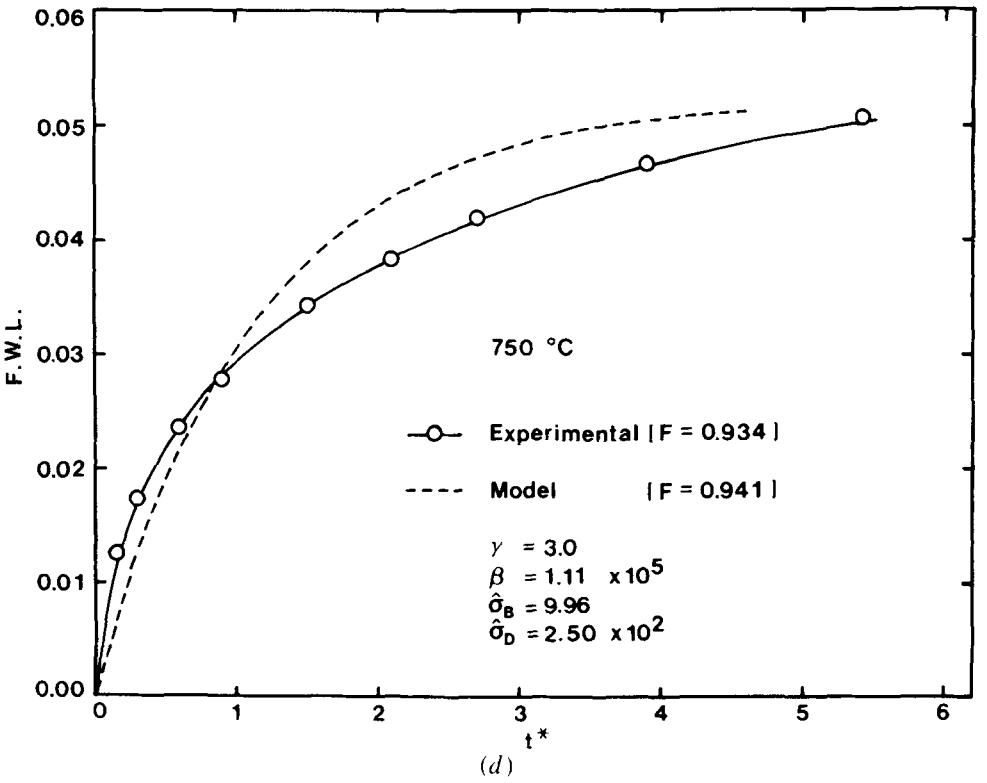

(*d*)

Fig 4—Comparison of the model predictions with experimental results at various temperatures (*a*) 600 °C, (*b*) 650 °C, (*c*) 700 °C, and (*d*) 750 °C

Figure 5 shows the predicted concentration profiles of H_2, H_2S, and H_2O within the pellets at a certain time ($t^* = 0.01$). These profiles are presented for the purpose of giving a qualitative picture of the concentrations at different temperatures. It should be noted that gaseous concentrations are plotted using different scales. As expected, the concentration of H_2S within a pellet is very low compared with those of H_2 and H_2O since the equilibrium concentration of H_2S is very small. Furthermore, the concentration of H_2O is considerably lower than that of H_2, thus justifying the assumption of pseudobinary diffusion made earlier. At a low temperature (a smaller value of $\hat{\sigma}_B$), diffusion of the gaseous species is much faster than the chemical kinetics, and the concentration of hydrogen is nearly uniform throughout the pellet and close to that in the bulk. The concentration of hydrogen sulfide is similarly uniform and close to that in the bulk. At higher temperatures (large values of $\hat{\sigma}_B$), the effect of hydrogen diffusion becomes greater.

Partially reacted pellets were sliced and examined under a scanning electron microprobe. No distinct compositional interfaces were found within the pellets reacted in the temperature range studied. Thus, it is believed that the resistance presented by chemical reaction and intrapellet diffusion are of comparable magnitude and the reaction takes place over a diffuse reaction zone (containing partly reacted particles) under conditions studied in this work.

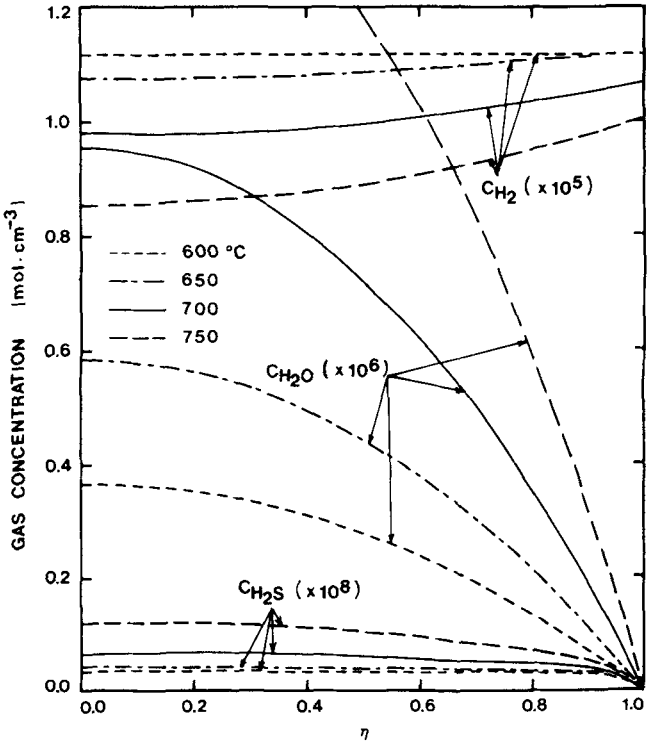

Fig. 5—Predicted gas-concentration profiles in the pellet ($t^* = 0.01$; $D_p = 0.829$ cm; $\varepsilon = 0.345$; $\gamma = 3.0$).

B. *Effect of Porosity*

In Figures 6(a) and (b), the results of the model are compared with experimental results using pellets of different porosities. The agreement is quite satisfactory. The higher porosity pellet ($\varepsilon = 0.531$) had a lower sulfur fixation ($F = 0.816$). This is due to the relatively fast diffusion of hydrogen sulfide in the more porous pellet. Thus, a smaller amount of H_2S reacts with lime, and the efficiency of lime in removing sulfur decreases with increasing porosity.

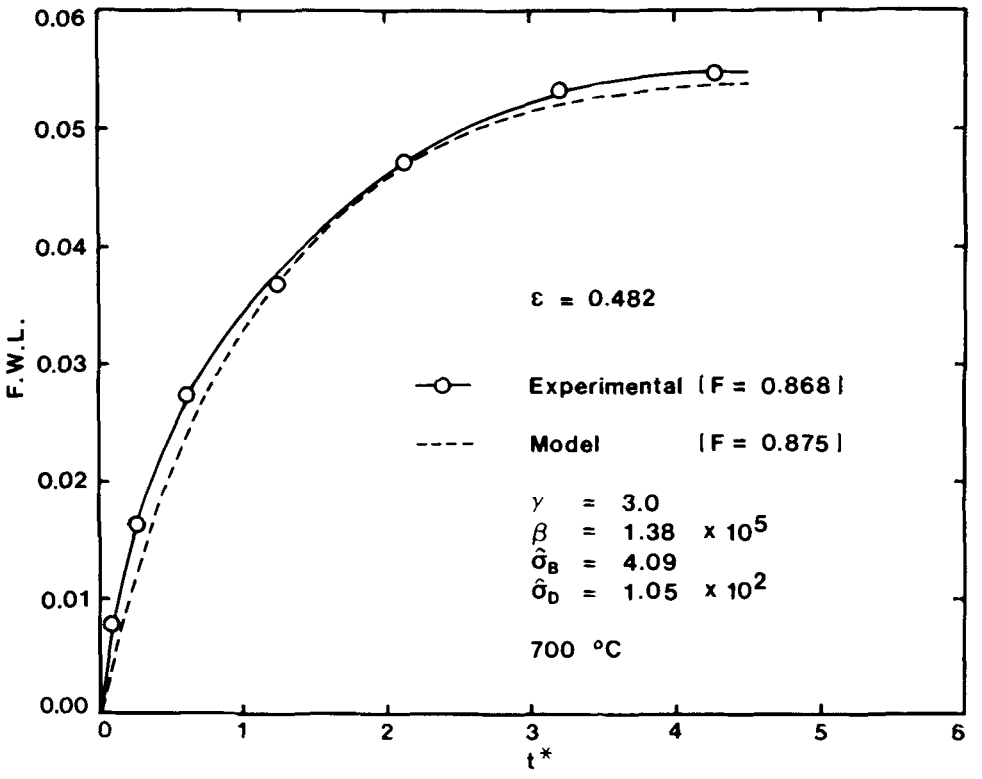

(*a*)

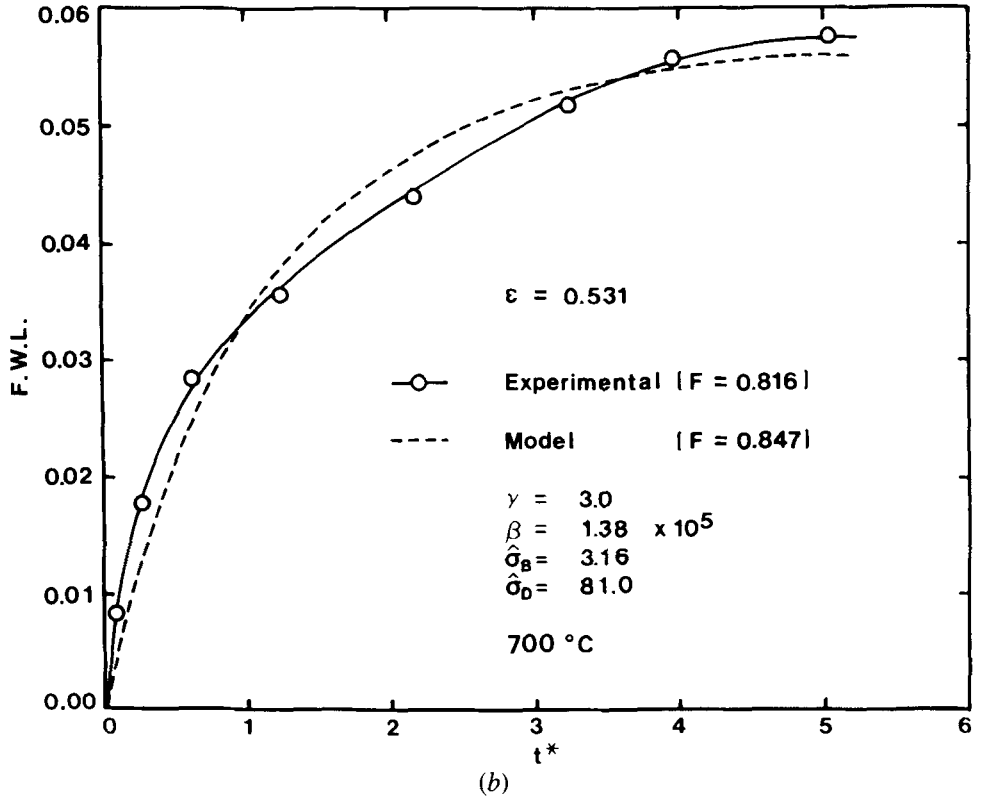

(*b*)

Fig. 6—Comparison of the model predictions with experimental results for pellets of different porosities. (*a*) $\varepsilon = 0.482$, (*b*) $\varepsilon = 0.531$

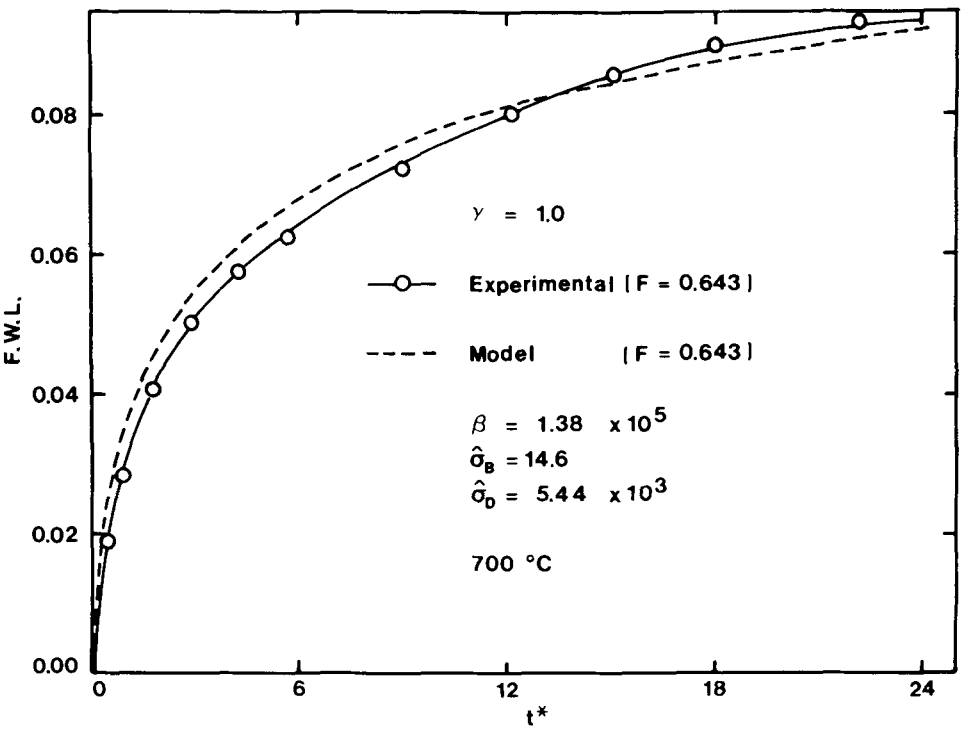

(a)

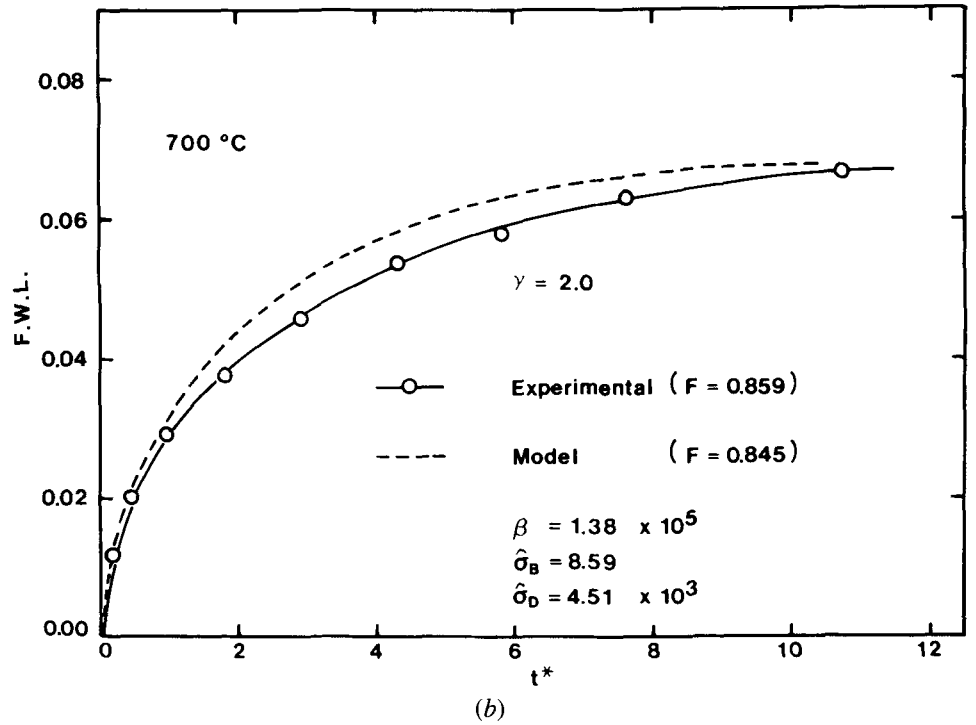

(b)

Fig 7—Comparison of the model predictions with experimental results for pellets of various solid mixing ratios: (a) $\gamma = 1.0$, (b) $\gamma = 2.0$, and (c) $\gamma = 4.0$

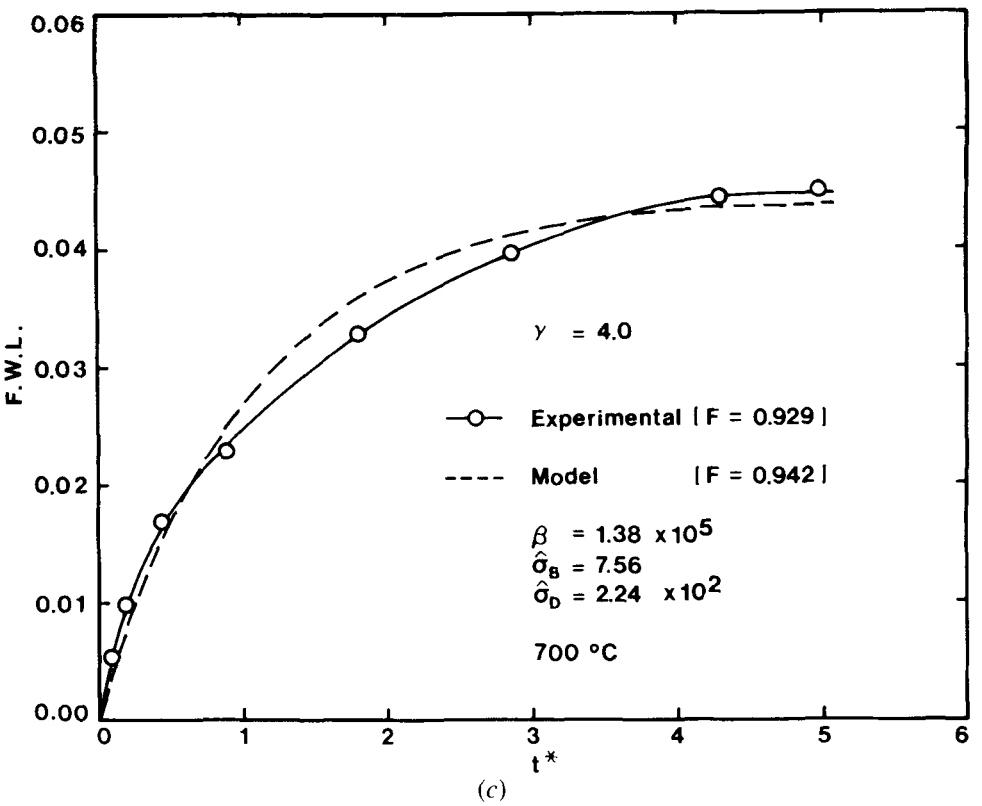

(*c*)

Fig. 7—Comparison of the model predictions with experimental results for pellets of various solid mixing ratios. (*a*) $\gamma = 1.0$, (*b*) $\gamma = 2.0$, and (*c*) $\gamma = 4.0$

C. *Effect of Mixing Ratio*

As shown in Figures 7(a) through (c), reasonable agreement between the model predictions and the experimental results is obtained for different mixing ratios. It is shown that, even for a large value of $\hat{\sigma}_B$ (= 14.6 for $\gamma = 1.0$), a substantial fraction of H_2S may escape from the pellet without reacting with lime unless an excess amount of lime is used. As discussed elsewhere,[14] the hydrogen sulfide reaction with lime slows down rapidly after the initial period of the reaction, and the remaining lime is not readily accessible to hydrogen sulfide gas. For this reason, although the value of $\hat{\sigma}_D$ for $\gamma = 1.0$ was slightly higher than that for $\gamma = 2.0$, the model prediction and experimental data for $\gamma = 1.0$ showed a substantially lower value of sulfur fixation.

D. *Effect of Pellet Size*

Since this set of experimental results was obtained using Cu_2S particles of different size (−150 +200 mesh), the intrinsic rate constant for reaction [1] was evaluated from the expression of nucleation and growth kinetics, in which the apparent rate constant is considered to be inversely proportional to the particle size of Cu_2S. This assumption is thought to be reasonable particularly in the case where the Cu_2S grains are approximately spherical and the hydrogen reduction of Cu_2S is of first order with respect to the solid reactant.[13]

The experimental results were in reasonably good agreement with the theoretical predictions as shown in Figures 8(a) through (c), which further justifies the assumption made regarding the effect of particle size in the rate constant. As the pellet diameter increased, the resistance due to intrapellet diffusion increased somewhat. Accordingly, the sulfur fixation increased.

E. *Effect of Variations of Parameters on the Model Predictions*

In view of the large number and different values of parameters that enter the computation, the computed results presented above were specific to particular, given experimental conditions. At this stage, it is thought desirable to discuss the effects of system parameters on the model predictions. For the purpose of providing an improved physical insight as to the overall reaction rate, the computed results given in the following figures are presented in terms of both F.W.L. and the conversion of chalcocite (X_B).

Inspection of Figure 9 shows that the reaction rate increases with temperature (t^* contains k_1, a function of temperature) and the sulfur fixation increases as the overall rate becomes more strongly affected by diffusion. There will be an optimum temperature to achieve a reasonable reaction rate and degree of sulfur fixation in the pellet.

As shown in Figure 10, the higher the porosity of the pellet, the higher the conversion of the sulfide with increasing H_2 diffusion rate, but the degree of sulfur fixation is lower as the diffusion rate of H_2S also increases. For a given temperature, pellet size, mixing ratio, *etc.*, there is an optimum porosity in terms of reduction rate and sulfur fixation.

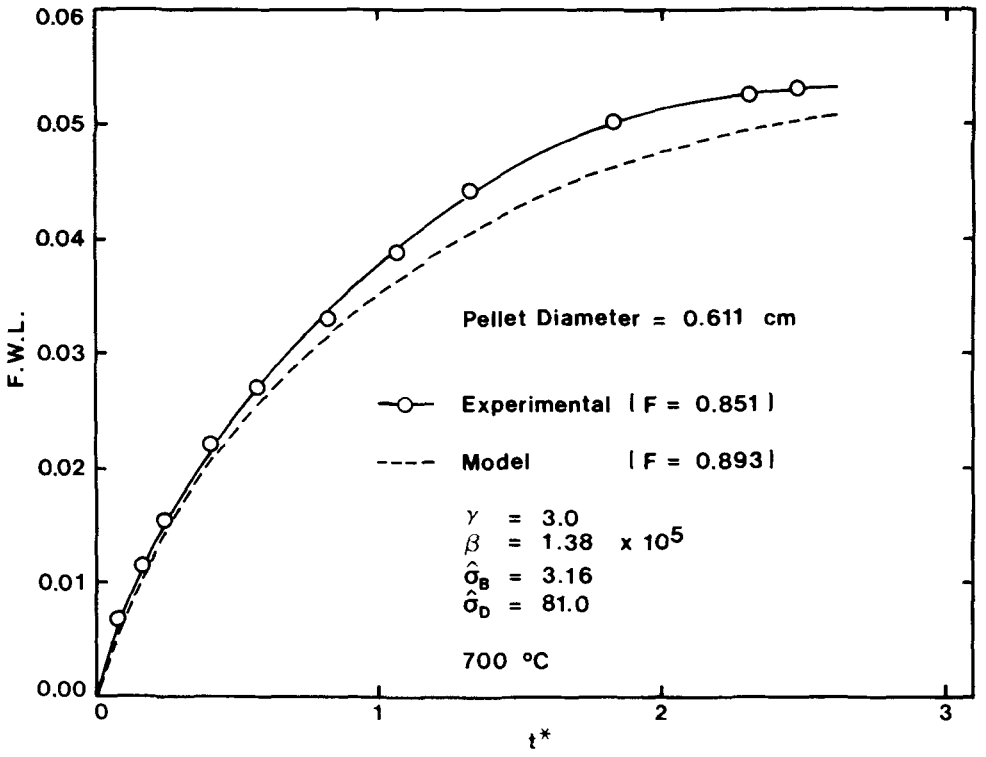

(*a*)

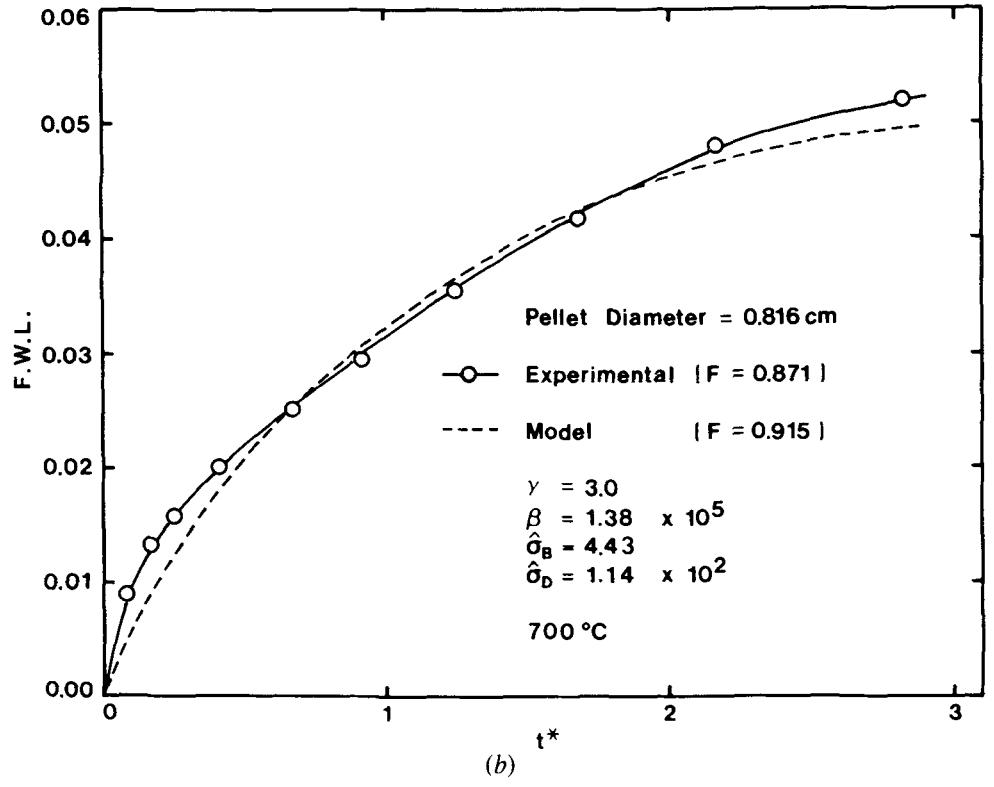

(*b*)

Fig. 8—Comparison of the model predictions with experimental results for pellets of various diameters (*a*) D_p = 0.611 cm, (*b*) D_p = 0.816 cm, and (*c*) D_p = 0.953 cm

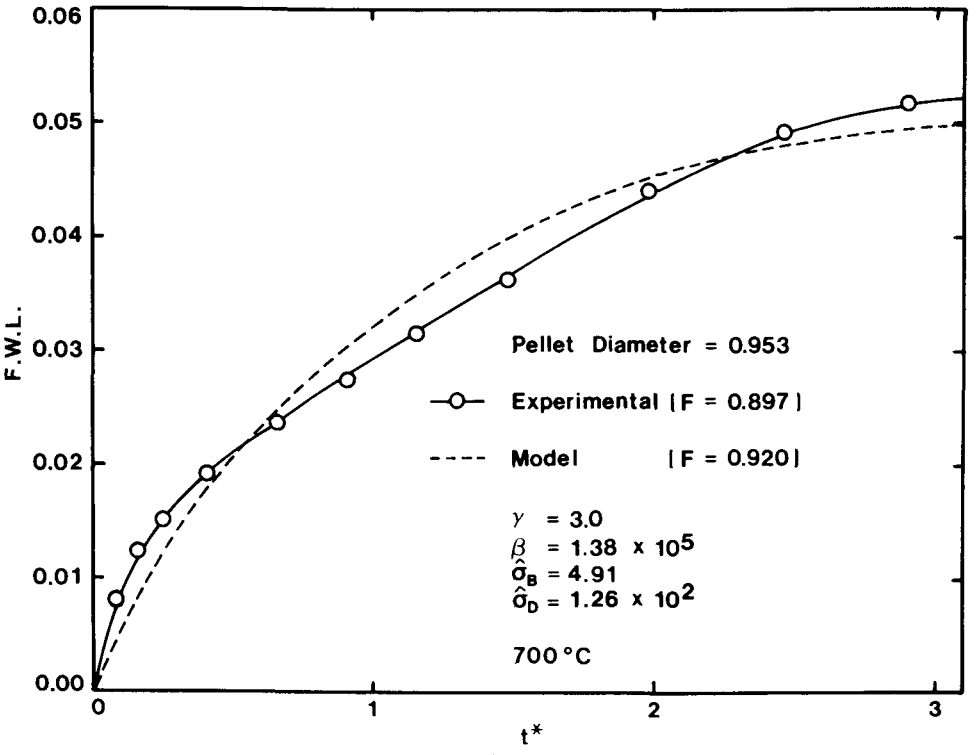

(c)

Fig 8—Comparison of the model predictions with experimental results for pellets of various diameters. (*a*) D_p = 0 611 cm, (*b*) D_p = 0.816 cm, and (*c*) D_p = 0.953 cm.

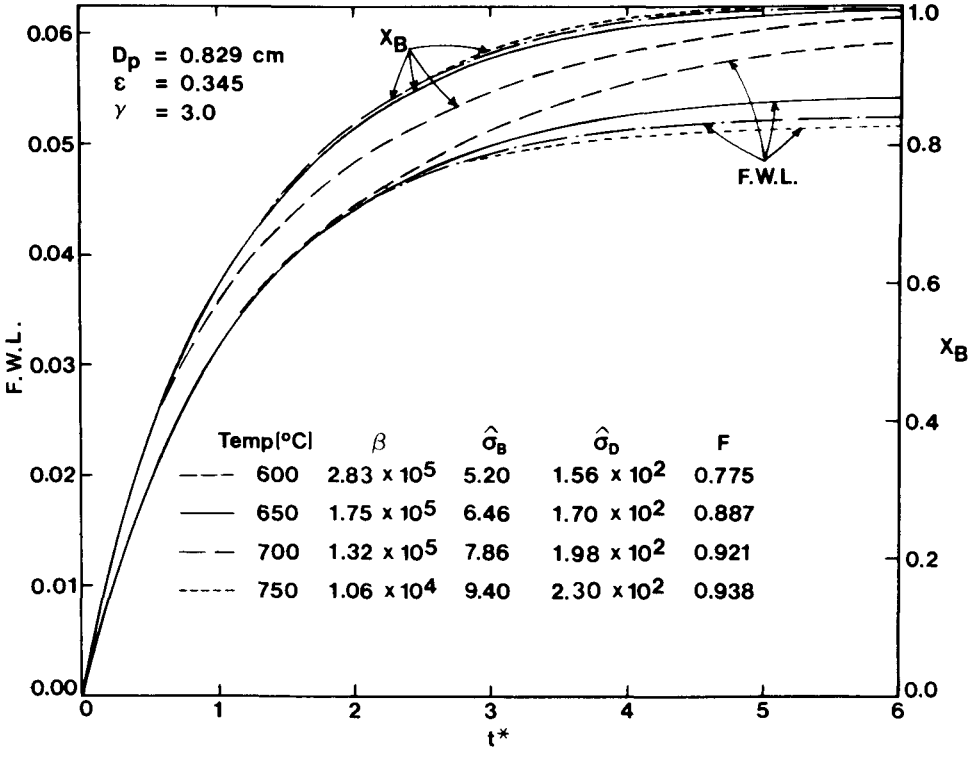

Fig. 9—Model predictions for the effect of temperature on conversion-vs-time relationships and sulfur fixation

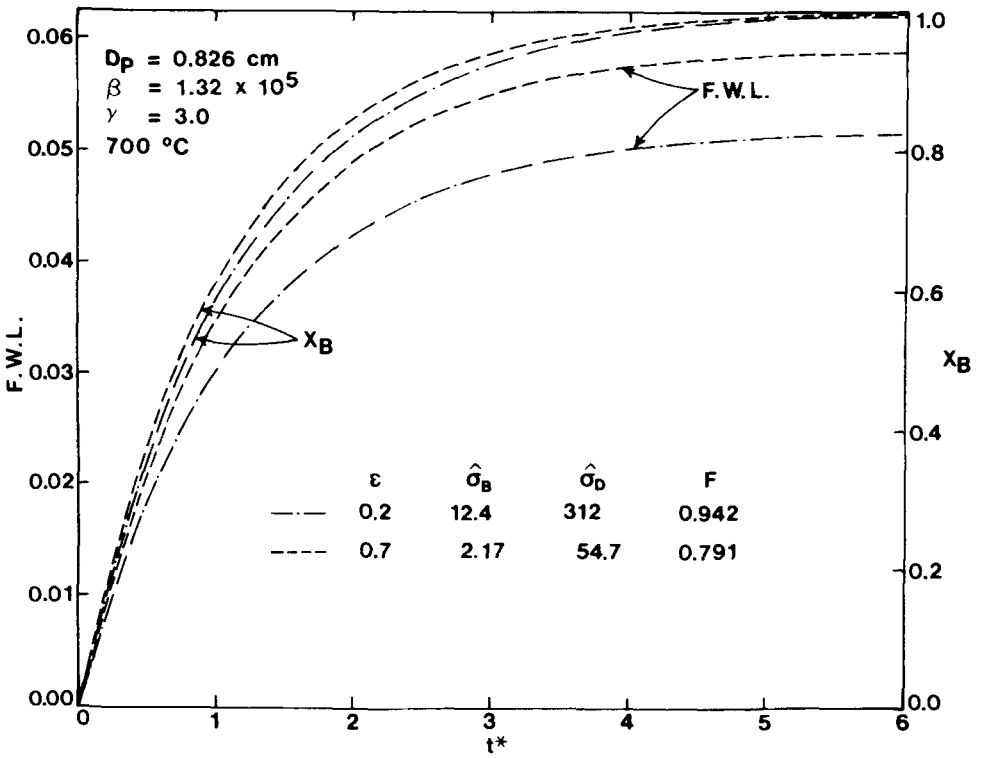

Fig. 10—Model predictions for the effect of porosity

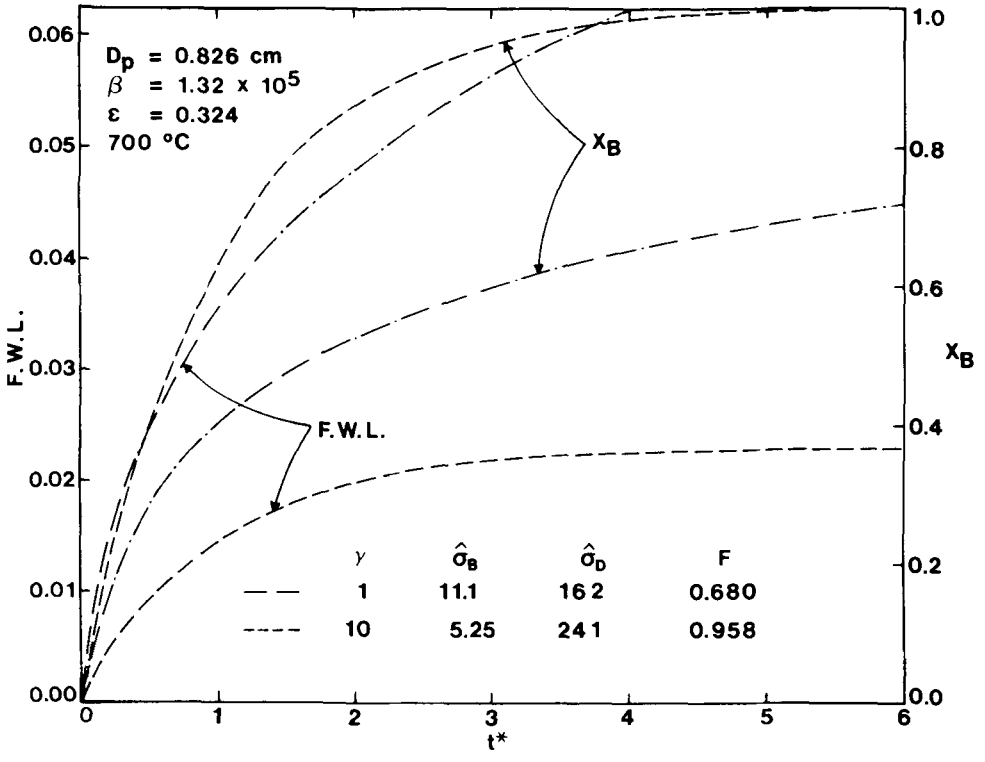

Fig. 11—Model predictions for the effect of solid mixing ratio

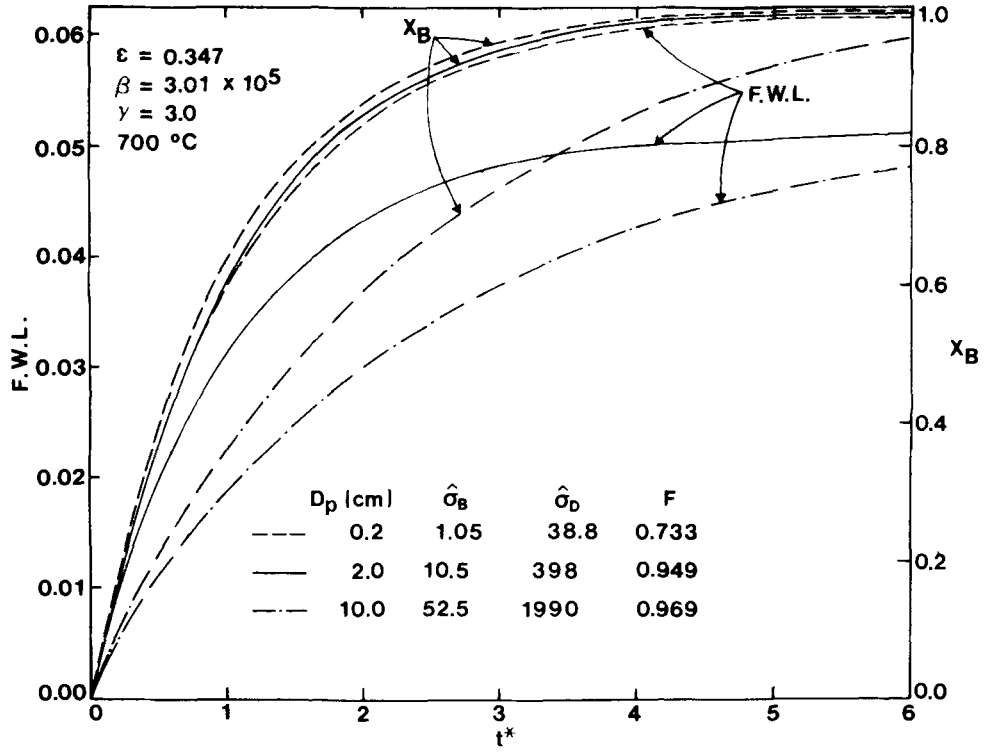

Fig. 12—Model predictions for the effect of pellet size

Increasing γ increases the extent of sulfur fixation in the solid and also speeds up the conversion of the sulfide, as seen in Figure 11. In most practical cases, however, there will be an optimum mixing ratio, above which excess lime becomes essentially an inert filler and slows down the overall rate of reaction per unit mass of the sulfide.

Figure 12 shows that, as the resistance due to intrapellet diffusion increases with pellet size, the reaction rate decreases but the sulfur fixation increases. There is an optimum pellet size which minimizes the diffusional resistance of hydrogen but provides a sufficient residence time for hydrogen sulfide within the pellet.

VII. CONCLUSIONS

A mathematical model of successive gas-solid reactions in a porous pellet has been applied to the hydrogen reduction of chalcocite in the presence of lime. The model was formulated incorporating basic physical and kinetic parameters. The physical parameters were measured experimentally except for the effective diffusivity which was estimated by using the measured physical properties. The kinetic parameters were obtained from the separate experiments of individual reactions: the hydrogen reduction of cuprous sulfide and the reaction of hydrogen sulfide with lime.

These parameters were incorporated into the theoretical model, the results of which were compared with the experimental results of the overall reaction in terms of both the conversion rate and the degree of sulfur fixation under different values of parameters such as temperature, porosity, mixing ratio, and pellet size.

The mathematical model was applied successfully to the hydrogen reduction of Cu_2S in the presence of lime except at a high temperature (750 °C) where extensive sintering took place. Knowledge of the sintering processes and their effect on diffusivities is limited at present. However, when such knowledge is available for a particular system, the model can easily be modified to take sintering into account. In all other runs, the deviation fell within ±10 pct of fractional weight loss and ±6 pct of sulfur fixation.

The model offers a means of determining the properties of an optimum pellet with a minimum number of experiments, which could be used for further scale-up applications. Furthermore, the model presented in this paper can be applied to hydrogen reduction of other sulfide minerals and for other successive reactions in general.

LIST OF SYMBOLS

A_p	External surface area of the pellet
b	Number of moles of solid B reacted per one mole of gas A in reaction [4]
c	Stoichiometry coefficient in reaction [4]
C_A, C_C, C_E	Concentrations of gases A, C, and E, respectively
C_{Ab}, C_{Cb}	Concentrations of gases A and C in the bulk, respectively
d	Stoichiometry coefficient in reaction [5]
D_e	Effective diffusivity in the porous solid
D_e, D_{eC}, D_{eE}	Effective diffusivities of gases A, C, and E, respectively
D_K	Knudsen diffusivity
D_M	Molecular diffusivity
D_p	Diameter of pellet
e	Stoichiometry coefficient in reaction [5]

F	Fraction of gas C captured by solid D, defined by Eq. [34]
F_p	Shape factor of the pellet (= 1, 2, and 3 for flat plates, long cylinders, and spheres, respectively)
k_1, k_2	Reaction rate constants for reactions [4] and [5], respectively
k_{20}	Preexponential factor of rate constant for reaction [5]
k_m	External-mass-transfer coefficient
K_1, K_2	Equilibrium constants for reactions [4] and [5], respectively
m	Constant defined in Eq. [9]
M	Atomic or molecular weight
r_c	Critical pore radius determined from pore size distribution of pellet
R	Distance coordinate in pellet
Sh*	Modified Sherwood number defined by Eq. [31]
t	Time
t^*	Dimensionless time defined by Eq. [27]
Δt^*	Dimensionless time step
T	System temperature
v_1, v_2	Net forward rates per unit volume of pellet of reactions [4] and [5], respectively
V_p	Volume of pellet
X_B, X_D	Overall conversions of solids B and D, respectively

Greek Symbols

α_B, α_D	Fractions of pellet volume initially occupied by solids B and D, respectively
β	Ratio of reactivities of solids D and B, defined by Eq. [26]
γ	Ratio of molar quantities of solids B and D defined by Eq. [25]
ε	Initial porosity of the pellet
η	Dimensionless distance coordinate in the pellet defined by Eq. [19]
λ	Constant defined in Eq. [10]
ρ_B, ρ_D	True molar densities of solids B and D, respectively
$\hat{\sigma}_B, \hat{\sigma}_D$	Generalized gas-solid reaction moduli for solids B and D, respectively, defined by Eqs. [22] and [23]
ψ_A, ψ_C	Dimensionless concentrations of gases A and C, respectively, defined by Eqs. [20] and [21]
ω_B, ω_D	Local values of the fractional conversions of solid reactants B and D, respectively

Other Symbols

∇^2, ∇^{*2}	The Laplacian operators with R and η, respectively, as the position coordinates

ACKNOWLEDGMENTS

This work was supported in part by the State of Utah Mineral Leasing Fund, by a grant from the University of Utah Research Committee, and by a Camille and Henry Dreyfus Foundation Teacher-Scholar Award Grant to H. Y. Sohn. The authors acknowledge with thanks a Graduate Fellowship to S. Won from the University of Utah Research Committee during this work, which was performed in partial fulfillment of the requirements for his Ph.D. degree.

REFERENCES

1. H Kay, in *High-Temperature Refractory Metals*, W A. Krivsky, ed., Gordon and Breach, New York, NY, 1968, pp 33-44
2. F. Habashi and R Dugdale *Metall. Trans* , 1973, vol. 4, pp. 1865-71.
3. J D Ford and M A Fahim, *Metall. Trans. B*, 1975, vol. 6B, pp 461-64
4. F. Habashi and B.I Yostos: *J Metals*, 1977, vol. 29, no 7, pp 11-16.
5. H.Y Sohn and K Rajamani, *Chem. Eng. Sci.*, 1977, vol. 32, pp. 1093-101
6. I.D. Shah and P.L. Ruzzi, *Metall Trans. B*, 1978, vol. 9B, pp 247-53.
7. P M Prasad and T.R. Mankhand, in *Advances in Sulfide Smelting*, Vol 1, Basic Principles, H Y Sohn, D B. George, and A.D. Zunkel, eds., 1983, pp 371-92.
8. K. Rajamani and H.Y. Sohn, *Metall. Trans B*, 1983, vol 14B, pp 175-80
9. M A Fahim, N. Wakao, and J. D. Ford: *Can. J Chem. Eng.*, 1978, vol 56, pp 725-29
10. M. A Fahim and J.D Ford *Can. J. Chem. Eng* , 1978, vol 56, pp 730-34.
11. K B. Bischoff: *Chem. Eng Sci.*, 1963, vol. 18, pp 711-13
12. D. Luss: *Can. J. Chem. Eng.*, 1968, vol. 46, pp. 154-56.
13. S Won, Ph D. Dissertation, University of Utah, Salt Lake City, UT, 1979
14. S Won and H Y Sohn: *Metall Trans B*, 1985, vol 16B, pp 163-68.
15. H Y Sohn and J Szekely: *Chem Eng Sci* , 1972, vol. 27, pp 763-78
16. J. Szekely, J W. Evans, and H.Y Sohn, *Gas-Solid Reactions*, Academic Press, New York, NY, 1976.
17. H Y Sohn *Metall Trans B*, 1978, vol. 9B, pp 89-96
18. H Y. Sohn and R L Braun, *Chem Eng Sci.*, 1980, vol. 35, pp 1625-35.
19. H.Y Sohn and R L Braun: *Chem Eng. Sci* , 1984, vol 39, pp 21-30
20. J Newman: *Ind Eng. Chem. Fundam* , 1968, vol. 7, pp. 514-17.
21. S Won and H.Y Sohn: *Trans. Inst Mining Metall.*, in press.
22. K K Kelley U S. Bur Mines Bull. 601, 1962
23. J F Elliott and M. Gleiser: *Thermochemistry for Steelmaking*, Addison-Wesley, London, 1960, vol 1
24. N Wakao and J.M Smith: *Chem. Eng Sci* , 1962, vol. 17, pp 825-34.
25. E A. Mason, A P. Malinauskas, and R.B Evans *J Chem Phys.*, 1967, vol. 46, pp. 3199-216.
26. C.N Satterfield, *Mass Transfer in Heterogeneous Catalysis*, M I.T Press, Cambridge, MA, 1970
27. R C. Reid, J M Prausnitz, and T K. Sherwood. *The Properties of Gases and Liquids*, 3rd ed., McGraw-Hill, New York, NY, 1977.